

Supplementary Information

A biomimetic wettability surface with switchable contact angle and adhesion for transfer and storage of microdroplets

Hanpeng Gao,^a Yan Liu,^{*a} Shuyi Li,^a Guoyong Wang,^b Zhiwu Han^a and Luquan Ren^a

^aKey Laboratory of Bionic Engineering (Ministry of Education), Jilin University, Changchun 130022, P. R. China; ^bKey Laboratory of Automobile Materials (Ministry of Education) and College of Materials Science and Engineering, Jilin University, Changchun, 130022, P. R. China

Table S1. Roughness parameters at different surface.

Specimen	R _p (μm)	R _v (μm)	R _z (μm)	R _a (μm)	R _q (μm)
original	5.32 ± 0.5	5.93 ± 1.6	11.25 ± 0.7	0.93 ± 0.5	1.19 ± 0.6
Laser processing	26.15 ± 3.4	16.86 ± 2.6	43.01 ± 2.8	5.43 ± 0.7	6.82 ± 1.4
Etched	18.36 ± 2.7	13.40 ± 3.8	37.37 ± 3.3	3.93 ± 1.3	4.93 ± 1.3

As shown in Table S1, laser processing significantly improves the surface roughness compared to the original surface. By comparing the laser processing and chemical etched surfaces, it can be seen that the roughness is slightly reduced. The decrease in roughness may be due to chemical etching that destroys part of the regular array of mastoid.

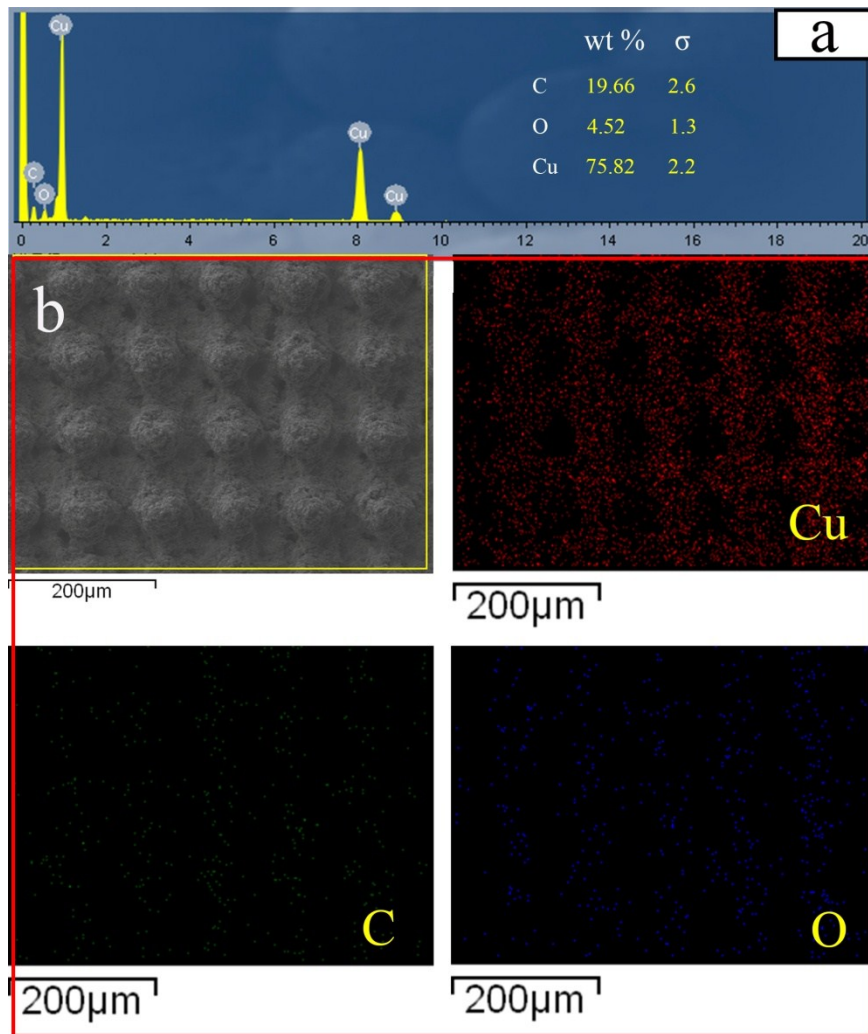


Fig. S1 (a) EDX results of the laser processing surface. (b) EDX element mapping of the selected area. The elements of Cu¹, C (green) and O (blue) appear on the surface. The scale bar is 200 μm .

The chemical composition of the laser processed surface was analyzed using EDX, as shown in Fig. S1a. The elements of Cu, C and O appear on the surface. The element of Cu was less distributed on the mastoid structures. And, the elements of C and O were mainly distributed on the mastoid structures (Fig. S1b).

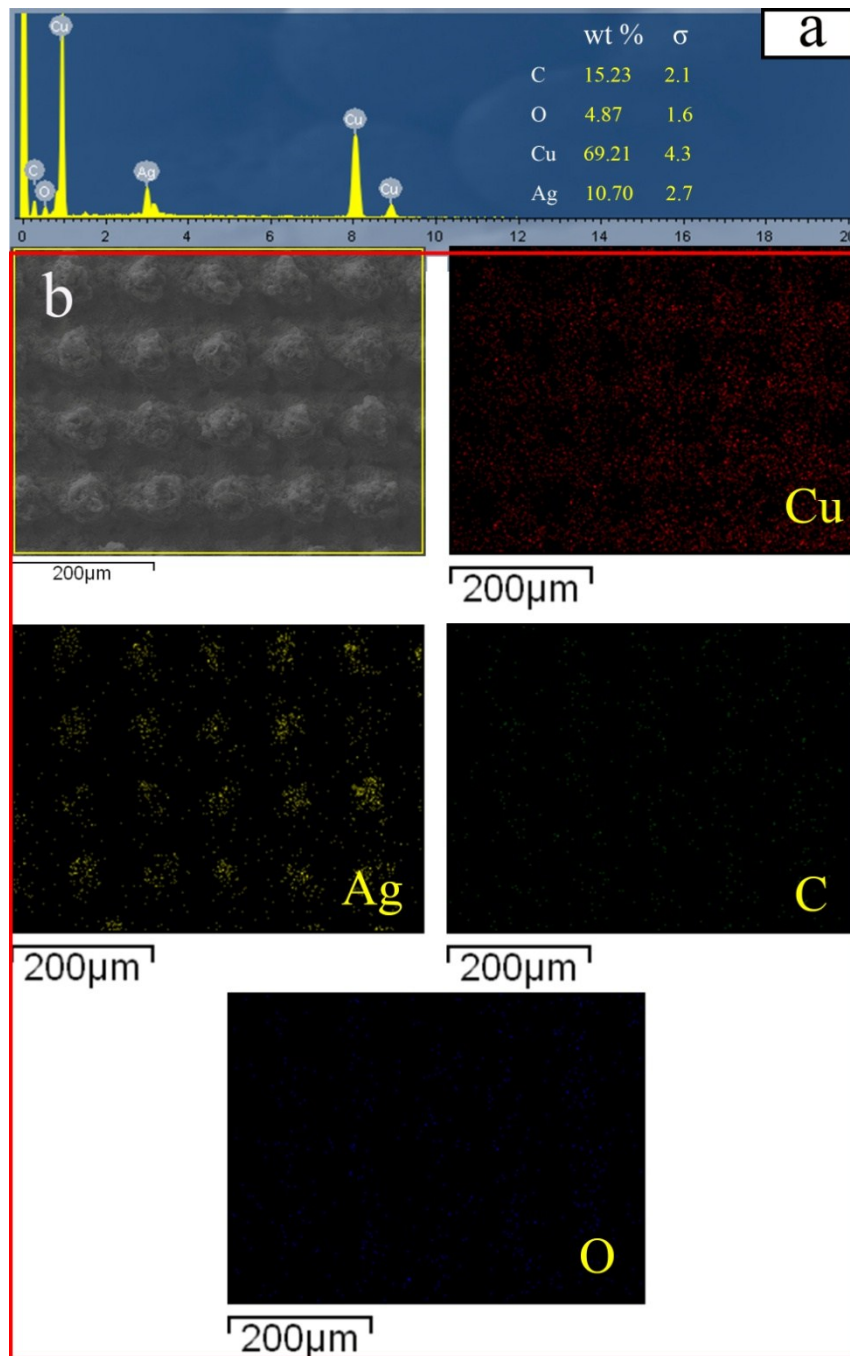


Fig. S2 (a) EDX results of the chemical etching surface. (b) EDX element mapping of the selected area. The elements of Cu¹, Ag (yellow), C (green) and O (blue) appear on the surface. The scale bar is 200 μm.

The chemical composition of the chemical etching surface was analyzed using EDX, as shown in Fig. S2a. The elements of Cu, Ag, C and O appear on the surface. The element of Cu was less distributed on the mastoid structures. And, the elements of Ag, C and O were mainly distributed on the mastoid structures (Fig. S2b). Based

on the principle of displacement reaction, it can be speculated that copper etching and silver adhesion occur simultaneously on the surface after soaking in silver nitrate.

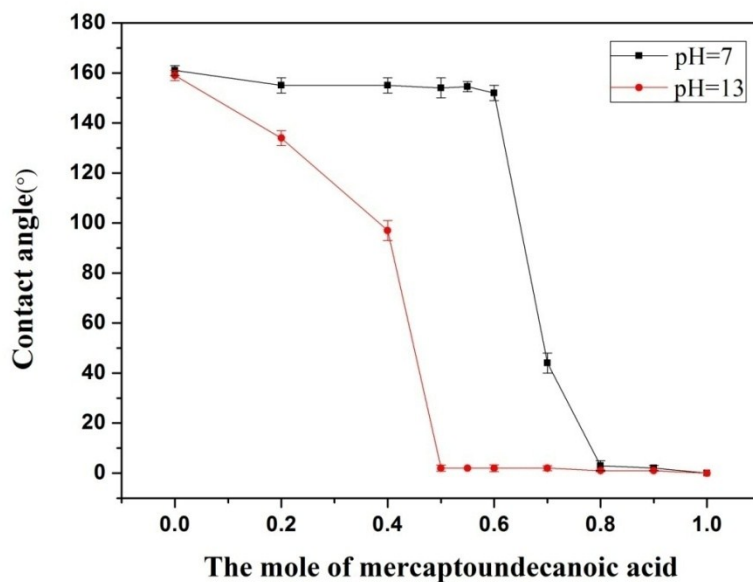


Fig. S3. Contact angle as a function of the molar ratio of 11-mercaptoundecanoic acid for neutral (pH = 7) and alkaline (pH = 13) droplets on the as-prepared surface.

The molar ratio of 1-Dodecanethiol and 11-Mercaptoundecanoic acid was very important for the pH-responsive surface. As shown in Fig. S3, when the molar fraction of 11-Mercaptoundecanoic acid was from 0.5 to 0.6, as-prepared surface can be transformed from superhydrophobicity to superhydrophilicity at different pH values. It was found that the increase in the number of moles 11-Mercaptoundecanoic acid would increase the response speed. Finally, we decided that the molar ratio of 11-Mercaptoundecanoic acid was 0.6 (total mixture concentration was $1 \text{ mM} \cdot \text{L}^{-1}$).

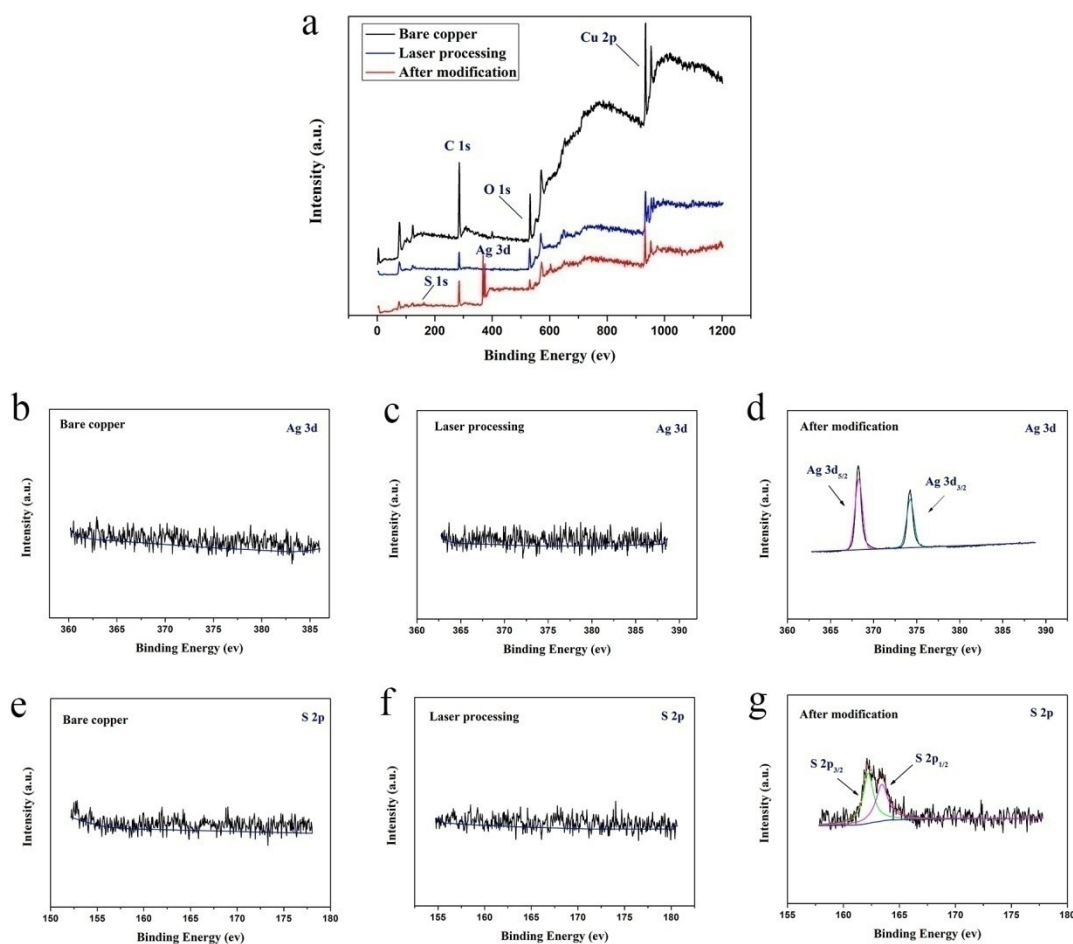


Fig. S4. (a) XPS survey spectra of bare copper (black), laser processed copper before (blue) and after modified by mixed solution ¹. XPS spectra of Ag 3d: (b) bare copper, (c) laser processing copper and (d) after modification copper. XPS spectra of S 2p: (e) bare copper, (f) laser processing copper and (g) after modification copper.

The chemical composition of the bare copper surface, laser processing copper surface and modification copper surface were investigated by XPS, respectively. The wide-scan spectra of the different surfaces in Fig. S4a show that Ag and S peak appear on the modification surface. Further, we analyzed the spectra of Ag 3d and S 2p on different surfaces. The Ag 3d peak did not appear on the original copper surface and laser processing copper surface (Fig. S4b and Fig. S4c). The peak of Ag 3d_{5/2} (368.26 eV) and Ag 3d_{3/2} (374.26 eV) appeared on the modification surface (Fig. S4d), which was consistent with zero-valent silver ($\Delta = 6.0$ eV).^{2, 3} This clearly confirms the formation of Ag on the processed copper surface. In addition, the S 2P peak did not appear on the original copper surface and laser processing copper surface (Fig. S4e

and Fig. S4f). The peak at S 2P_{3/2} (162.22 eV) and S 2P_{1/2} (163.44 eV) appeared on the modification surface (Fig. S4g).^{4, 5} The results show that the mixed thiols combine with the metal surface. However, this combination mechanism needs further confirmation. Therefore, we used FT-IR to further study the as-prepared surface.

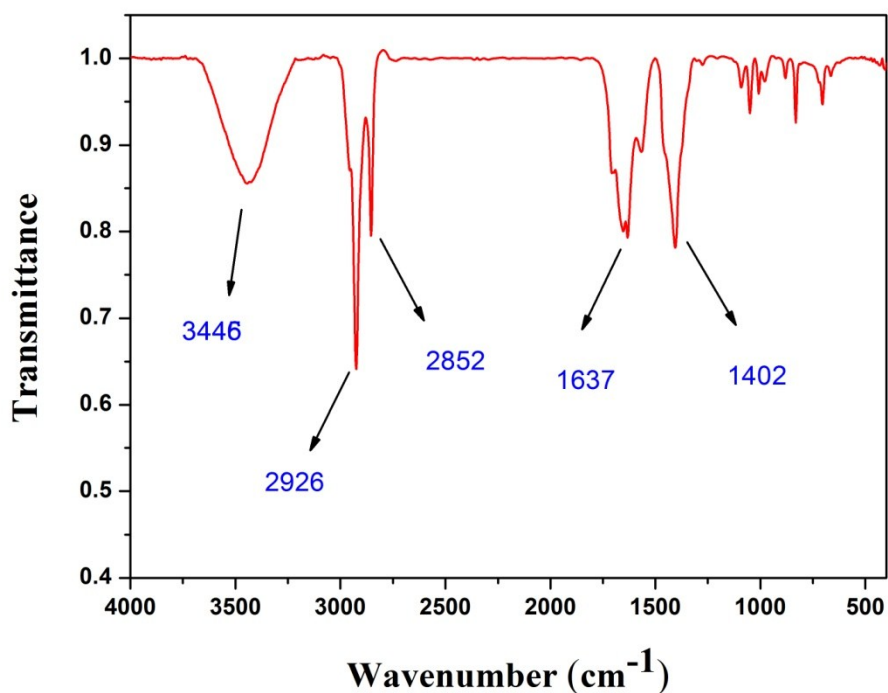


Fig. S5. FT-IR spectra of the as-prepared copper surfaces modified by mixed solution.

In order to confirm the combination mechanism of the mixed solution on the as-prepared surface, FT-IR spectra was used (Fig. S5). The adsorption peaks at about 3446 cm⁻¹ were due to O–H stretching vibration and the adsorption peaks at 1637 cm⁻¹ are ascribed to C=O stretching vibration. The adsorption peaks at 1402 cm⁻¹ are ascribed to –S–C– stretching vibration (it can be attributed to mixed thiols). The band at 2852 cm⁻¹ is attributed to the long chains –(CH₂)_n of HS(CH₂)₁₀COOH and HS(CH₂)₁₁CH₃. The band of –CH₃ from HS(CH₂)₁₁CH₃ appears at 2926 cm⁻¹.

The combination of thiols and the as-prepared surface can be further explained by the following formula:⁶





The RSH stands for thiol. And the M stands for metal, including copper, silver or gold. These results indicate that the prepared surface was successfully modified with mixed thiols.



Fig. S6. The contact angle of the oil droplets on as-prepared surface.

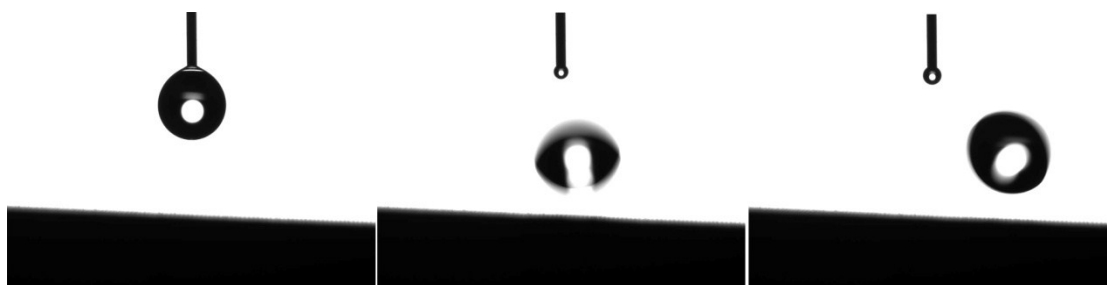


Fig. S7. The as-prepared superhydrophobic surface has a sliding angle of $\sim 3^\circ$, showing a low adhesion.

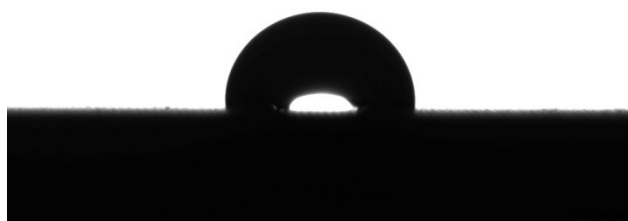


Fig. S8. The contact angle of the ink was completely covered on as-prepared superhydrophobic surface. The contact angle was $94.5 \pm 2^\circ$.

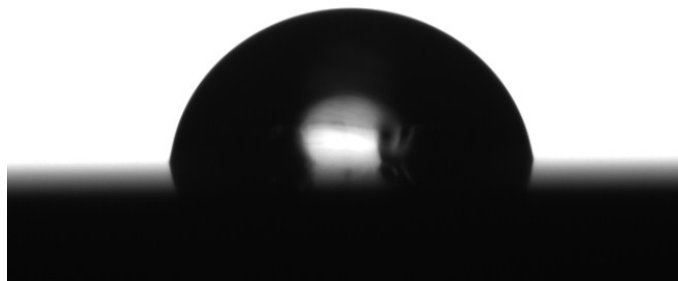


Fig. S9. The contact angle of bare copper (after polish, 83.8°).

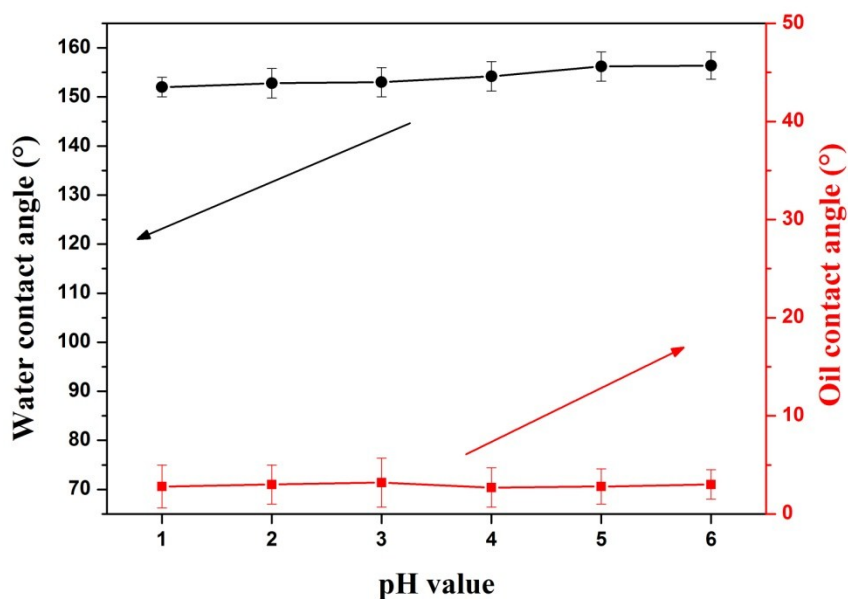


Fig. S10. Water contact angles and underwater oil contact angles of the as-prepared copper surface as a function of different water pH values.

With the decrease of pH, the contact angle of water droplets was slightly reduced (Fig. S10). In other words, under acidic conditions, the surface does not have the ability to regulate wettability. This is because the carboxyl group is protonated under acidic conditions, which allows the surface to remain superhydrophobic.



Fig. S11. The template used to precisely control the size of the ink dots, which was obtained by laser processing (the diameters were 0.6 mm, 0.9 mm 1.2mm and 1.5 mm, respectively).

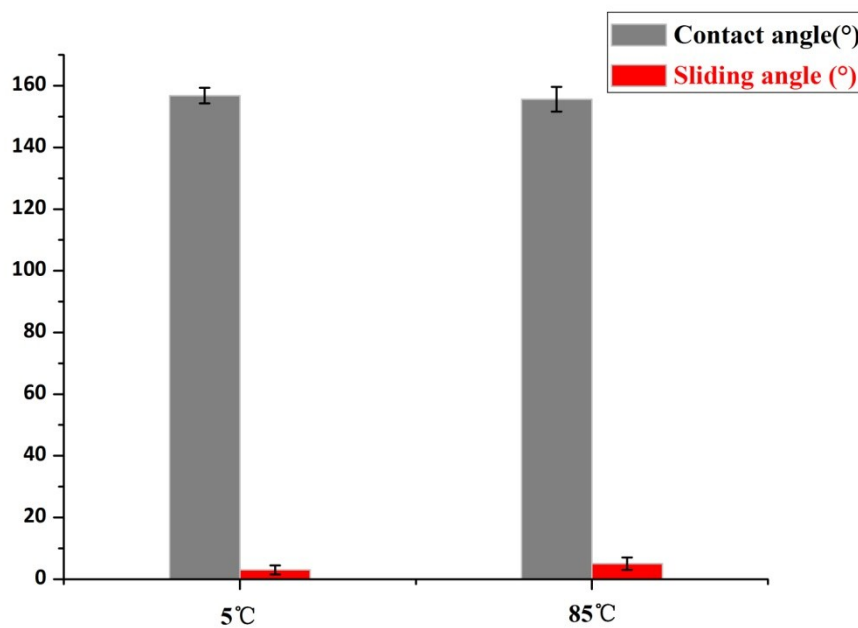


Fig. S12 Contact angles or sliding angles of as-prepared surface as a function of the different droplet temperature.

The contact angle and sliding angle of as-prepared surface did not change significantly as the droplet temperature was raised (85 °C) or lowered (5 °C). This means that as-prepared surface can manipulate droplets of different temperatures (5 °C or 85 °C).

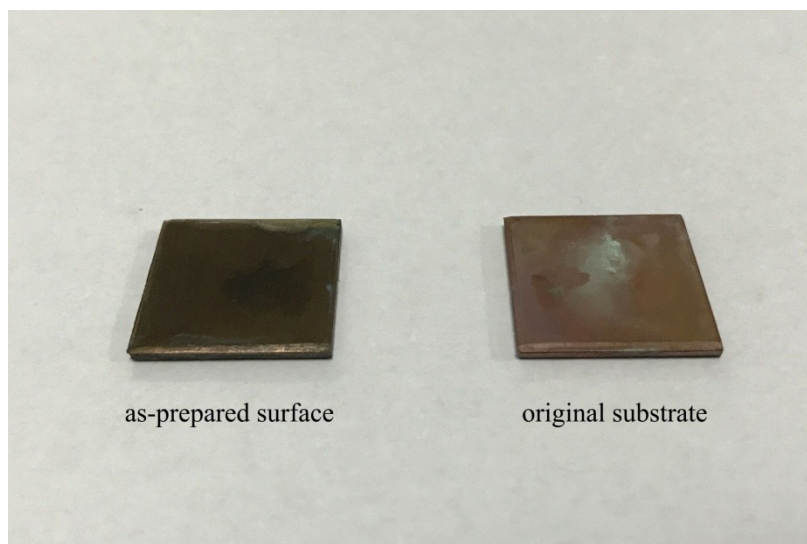


Fig. S13 Photographs of as-prepared surface and original substrate after 7 days of salt spray test.

In order to study the corrosion resistance of the as-prepared surface under corrosive liquid vapour, the salt spray experiment was used to test the surface. The test conditions were ambient temperature of 35 °C and the corrosive solution was 50 g/L NaCl aqueous solution. After 7 days, corrosion was found on both the as-prepared surface and the original substrate. Unlike liquid corrosion, the as-prepared surface will be in direct contact with the corrosive liquid vapour and does not exhibit good corrosion resistance. Although some studies have shown that the self-assembled molecular layer of thiol molecules on the metal surface also has an inhibitory effect on corrosion, such corrosion resistance is not obvious in our salt spray test. Therefore, due to the corrosion resistance mechanism, the corrosion resistance of the as-prepared surface has certain limitations.

References

1. T. Darmanin and F. Guittard, *Prog. Polym. Sci.*, 2014, **39**, 656-682.
2. H. Peng, L. Yuan, J. Zhang, X. Wu, Y. Liu, Y. Liu and R. Ruan, *Carbohydr. polym.*, 2018, **188**, 8-16.
3. C. Yuan, W. Wei, Y. Mei, X. Luo and W. Lei, *Mater. Lett.*, 2017, **190**, 248-251.
4. B. Yang and A. G. Agrios, *J. colloid interf. sci.*, 2018, **513**, 464-469.
5. X. J. Hong, T. X. Tan, Y. K. Guo, X. Y. Tang, J. Y. Wang, W. Qin and Y. P. Cai, *Nanoscale*, 2018, **10**, 2774-2780.

6. E. L. Paul, M. W. George, L. A. David, T. Yu Tai, N. P. Atul and G. N. Ralph, *J. Am. Chem. Soc.*, 1991, **113**, 7152-7167.